DOI: https://doi.org/10.30795/jfootankle.2026.v20.2156

Special Article

Anatomical structures at risk in third- and fourth-generation minimally invasive hallux valgus surgery: A comprehensive review

Kepler Alencar Mendes de Carvalho[1,2], Samai Ferrarezi[1], Aly Fayed[1], Miki Dalmau-Pastor[2]

1. Department of Orthopedics and Rehabilitation, University of Iowa, Iowa City, IA, USA.
2. Human Anatomy and Embryology Unit, Experimental Pathology and Therapeutics Department, University of Barcelona, Spain.

Abstract

A critical limitation common to all minimally invasive surgery (MIS) approaches is the lack of direct visualization during osteotomy execution, which exposes arteries, nerves, and tendon insertions to iatrogenic injury within a confined anatomical space. This review synthesizes applied anatomical knowledge relevant to third- and fourth-generation MIS for hallux valgus (HV), incorporating findings from cadaveric dissection and micro-computed tomography (CT) vascular mapping to characterize the tendinous, neural, vascular, and sesamoid architecture of the first metatarsal head complex and to define quantitative safety zones for intraoperative reference. Micro-CT perfusion studies have established that the apex of the Chevron osteotomy should be positioned at a minimum distance of 25.6 mm (dorsal arm) and 23.9 mm (plantar arm) from the most distal point of the first metatarsal articular surface, with the excursion of the Shannon burr limited to 3.9 mm and 4.0 mm beyond the exit point on the lateral cortex. The Metaphyseal Extra-Articular Transverse and Akin Osteotomy (META) technique introduces a geometrically distinct risk profile by simultaneously addressing the dorsal and plantar metatarsal arteries in a single transverse plane; for this technique, a unified safety distance of approximately 26 mm is proposed for the osteotomy, pending specific anatomical application and micro-CT validation. Neurological risk for both osteotomy generations centers on the dorsomedial nerve of the first toe. Biomechanical and radiographic equivalence between third- and fourth-generation constructs indicates that the choice of technique should be guided by surgical training rather than perceived mechanical superiority, and that safe execution depends on mastering the anatomical boundaries described in this review.

Level of Evidence V; Expert Opinion, Basic Science Study.

Keywords: Hallux valgus; Minimally invasive surgical procedures; Osteotomy; Micro-CT scan; Nerve injury.

Introduction

Hallux valgus (HV) represents one of the most prevalent forefoot deformities, affecting an estimated 19% of the general population worldwide, with a marked female predominance and increasing prevalence with age[1,2]. The condition is a complex three-dimensional (3D) deformity characterized by a lateral deviation of the hallux at the first metatarsophalangeal joint (MTPJ), concurrent with medial deviation of the first metatarsal, and is associated with significant impairment of health-related quality of life, affecting gait, balance, footwear tolerance, and psychosocial well-being[1-4].

Surgical correction is the standard of care for symptomatic HV that has failed conservative management, with over 150 operative techniques described in the literature[5]. Among these, minimally invasive surgery (MIS) has gained substantial traction over the past two decades. Compared with traditi-

Study performed at the Department of Orthopedics and Rehabilitation, University of Iowa, Iowa City, IA, USA and Human Anatomy and Embryology Unit, Experimental Pathology and Therapeutics Department, University of Barcelona, Spain.

Correspondence: Kepler Alencar Mendes de Carvalho. Complete Address and Zip Code: **E-mail:** kepler-carvalho@uiowa.edu. Conflicts of interest: none. Source of funding: none. **Date received:** August 04, 2026. **Date accepted:** August 04, 2026.

How to cite this article: Carvalho KAM, Ferrarezi S, Fayes A, Dalmau-Pastor M. Anatomical structures at risk in third- and fourth-generation minimally invasive hallux valgus surgery: A comprehensive review. J Foot Ankle. 2026;20(2):e2156.

onal open procedures, MIS techniques offer smaller incisions, reduced soft tissue dissection, lower postoperative pain, earlier weight-bearing, and faster return to activity[6,7].

Minimally invasive surgery for HV has evolved through four successive generations. First-generation percutaneous techniques (e.g., Reverdin-Isham osteotomy) used intra-articular osteotomies without internal fixation, restricted to mild-to-moderate deformities. Second-generation techniques (e.g., Bösch technique) employed extra-articular transverse osteotomies stabilized with Kirschner wires, offering improved bone union but limited rotational control[8]. Third-generation minimally invasive techniques for HV correction, such as the Minimally Invasive Chevron-Akin (MICA) procedure described by Vernois and Redfern, combined a percutaneous, chevron-shaped distal metatarsal osteotomy with rigid fixation using two screws, providing sufficient intrinsic stability to allow early weight-bearing and substantial lateral translation of the metatarsal head, even in cases of severe deformity[9,10]. Variations of this concept, including the Percutaneous Intra-articular Chevron Osteotomy (PeICO) described by Del Vecchio et al.[11], replicate the geometry and angulation of the classic open Chevron osteotomy while requiring only a single screw for fixation. Fourth-generation techniques, as described by Lewis et al.[12] in the Metaphyseal Extra-articular Transverse and Akin Osteotomy (META), preserve the principle of rigid fixation with two fully threaded screws – at least one of which must be bicortical – but replace the Chevron geometry with a transverse, extra-articular osteotomy. This configuration is intentionally less stable at the osteotomy site, which permits an active three-dimensional reduction maneuver capable of correcting not only the intermetatarsal and hallux valgus angles but also the rotational (pronation) component of the deformity, a correction that Chevron-based designs are less able to achieve due to their inherent geometric stability[9-13].

A critical limitation inherent to all MIS approaches is the absence of direct visualization during osteotomy execution[13-15]. The Shannon burr operates within a confined anatomical space populated by major arterial pedicles, cutaneous nerves, and tendinous insertions – all of which are at risk of iatrogenic injury[14]. Paradoxically, the literature on MIS outcomes rarely characterizes these complications in detail, and quantitative data on safe distances from at-risk structures remain scarce.

This review synthesizes applied anatomical knowledge relevant to the practice of third- and fourth-generation MIS HV surgery, incorporating cadaveric dissection findings and micro-computed tomography (CT) vascular mapping. The objective is to provide the operating surgeon with a structured, evidence-based framework for understanding the anatomical risk zones and safe operating corridors when performing MIS third- and fourth-generation distal metatarsal osteotomies to treat HV deformities.

Applied anatomy of the first metatarsal head complex

The first metatarsal head complex encompasses a constellation of tendinous, ligamentous, neural, and vascular structures that converge upon the first metatarsophalangeal joint (MTPJ). Intimate knowledge of their spatial relationships is indispensable for safe MIS execution[16]. The relevant structures may be organized into four anatomical domains: tendons, nerves, blood supply, and the sesamoid complex[16].

Tendons of the first metatarsal head complex

The extensor hallucis longus (EHL)

The EHL muscle's primary function is hallux extension and ankle dorsiflexion. Its tendon insertion on the distal phalanx of the hallux also contributes to weak foot inversion. Originating on the fibula and inserting on the distal phalanx of the hallux, EHL contraction results in elevation of the foot and hallux toward the tibia. This action is essential for gait, enabling foot clearance during the swing phase. Injury to the deep peroneal nerve, which innervates the EHL, can lead to foot drop, characterized by weakened dorsiflexion and a characteristic high-stepping gait pattern (Figure 1A)[16-19].

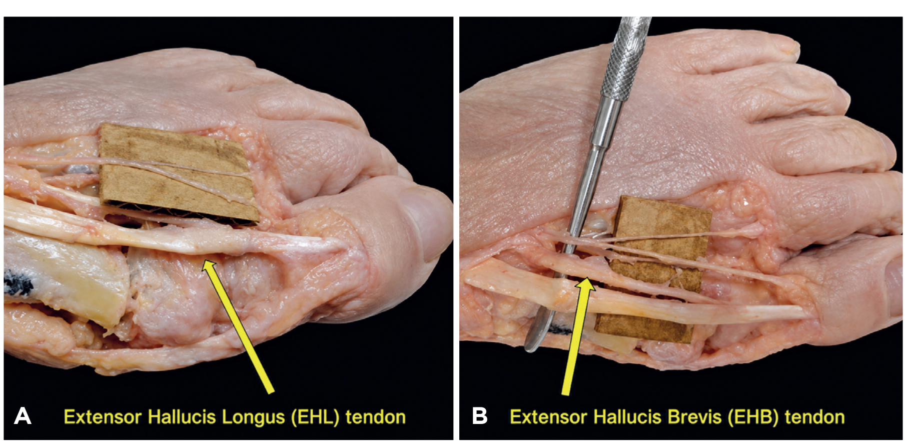

Figure 1. First metatarsal head dorsal aspect: (A) the extensor hallucis longus (EHL) and (B) the extensor hallucis brevis (EHB) tendons.
Source: Carvalho (2025)[16]

The extensor hallucis brevis (EHB)

The EHB is regarded as a distinct medial slip of extensor digitorum brevis. This muscle thus originates from the superolateral surface of the distal calcaneus, from the interosseous talocalcaneal ligament, and from the deep aspect of the base of the inferior extensor retinaculum. Its tendon inserts onto the dorsal surface of the base of the proximal hallucal phalanx (Figure 1B). It is innervated by the deep fibular (peroneal) nerve[16,20].

The flexor hallucis longus (FHL)

The FHL muscle originates from the posterior aspect of the fibula. Its tendon courses through the tarsal tunnel, passing inferior to the medial malleolus of the tibia, and inserts onto the distal phalanx of the hallux (Figure 2)[16,21,22]. The FHL's primary action is flexion of the hallux. It also contributes to plantar-medial force distribution within the forefoot, providing support to the medial longitudinal arch[16,23].

The flexor hallucis brevis (FHB)

The FHB, an intrinsic muscle of the foot, originates along the plantar aspect of the cuboid and cuneiform bones[16,24]. The FHB divides distally into two portions that are inserted on the medial and lateral aspects of the base of the proximal phalanx of the hallux. The medial head of the FHB, the larger of the two, inserts medially on the plantar plate and shares a common tendon with the abductor hallucis muscle prior to its insertion on the base of the proximal phalanx[16,25]. An accurate understanding of this insertion is critical in surgical procedures involving the first MTPJ, particularly those addressing HV[16,26].

The abductor hallucis (AH)

The AH is the most superficial muscle in the medial compartment of the first layer of the plantar aspect of the foot, has a proximal attachment primarily to the flexor retinaculum and posterior calcaneal tuberosity, with some fibers also attaching to the intermuscular septum separating it from the FHB[16,27,28]. Distally, its tendon inserts onto the base of the proximal phalanx of the hallux (Figure 3A). Innervated by a branch of the medial plantar nerve and supplied by a branch of the medial plantar artery, the AH contributes to maintaining the medial longitudinal arch of the foot. Muscle contraction results in abduction of the hallux[16,20,27,28].

The adductor hallucis

The adductor hallucis muscle, composed of the oblique and transverse heads, is responsible for the adduction of the great toe[29]. The transverse head arises from the ligaments associated with the MTPJ of the three lateral toes. In contrast, the oblique head arises from the bases of metatarsals II through IV and the sheath covering the peroneus longus tendon (Figure 3B)[29]. According to Sarrafian's[30] description of the insertion of the adductor hallucis, the distal segment of the oblique head consists of three components, each attaching to the fibular sesamoid, with the lateral component extending to the plantar lateral aspect of the base of the proximal phalanx[30,31]. Its action is adduction of the great toe at the MTPJ. The adductor hallucis receives its arterial supply from the lateral plantar artery and is innervated by the lateral plantar nerve, a branch of the tibial nerve[29,32]. Knowledge of this anatomical configuration highlights the potential risk of injury during surgical correction of the HV when performing a release along the base of the proximal phalanx[16].

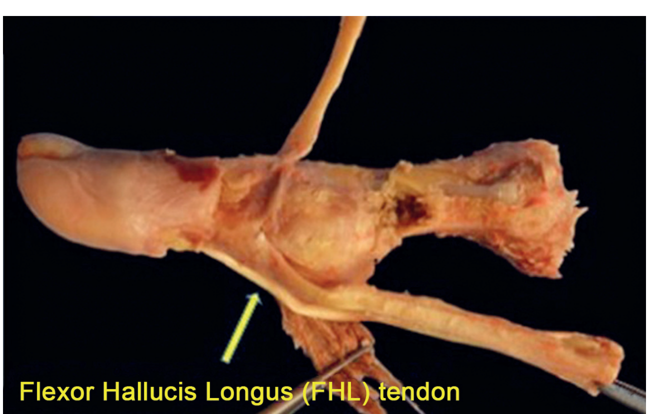

Figure 2. First metatarsal head plantar aspect: The flexor hallucis longus (FHL) tendon.
Source: Carvalho (2025)[16]

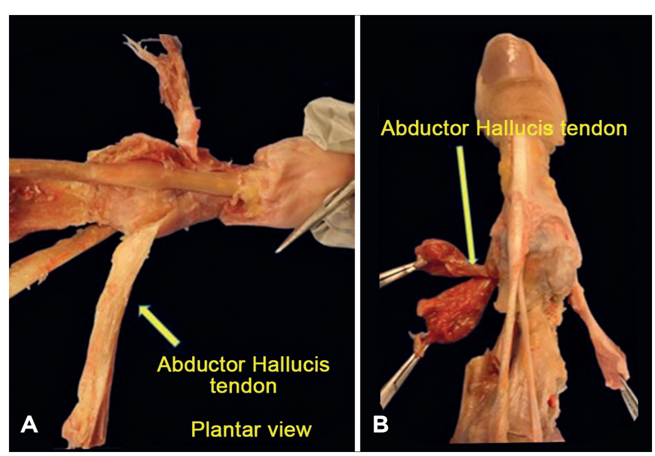

Figure 3. First metatarsal head medial aspect: (A) the abductor hallucis tendon. First metatarsal head lateral aspect: (B) the adductor hallucis tendon.
Source: Carvalho (2025)[16]

Nerves of the first metatarsal head complex

Iatrogenic injury to subcutaneous nerves on the dorsum of the foot is an established risk factor during surgical procedures, including HV correction, resulting in postoperative pain, sensation loss, and painful neuroma[16,33-36].

The deep peroneal nerve (DPN) and the superficial peroneal nerve (SPN) arise from the common peroneal nerve that supplies the skin on the distal anterior aspect of the leg and the dorsal aspect of the foot[16,31,37]. The DPN innervates the skin at the interdigital space between the first and second toes, and the SPN innervates the remaining part of the dorsum of the foot[16,35].

The dorsomedial nerve of the first toe and its medial branch emerge from SPN, and the dorsolateral nerve of the first toe and the dorsomedial nerve of the second toe emerge from DPN (Figure 4)[16,33,34].

Blood supply of the first metatarsal head complex

The extrinsic vascular supply to the first metatarsal originates from the first dorsal metatarsal artery (FDMA), the lateral dorsal branch of the FDMA, and the first plantar metatarsal artery (FPMA). These arteries give rise to localized branches within the first metatarsal, which further subdivide into smaller arteries surrounding the periosteum and joint capsule[14,16,30,31,38].

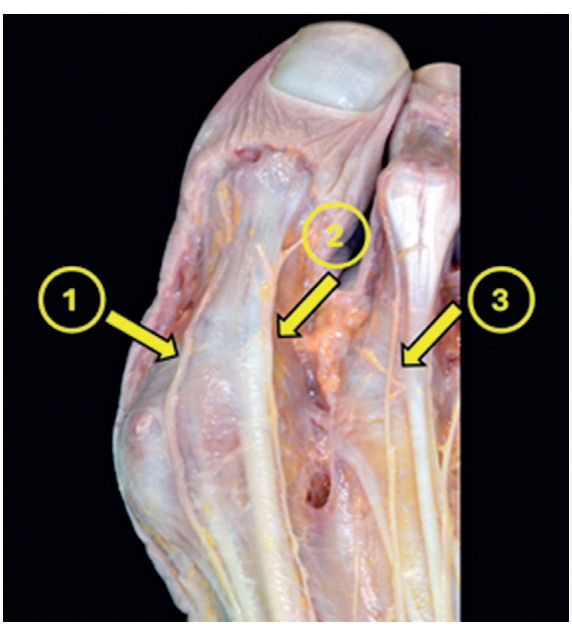

Figure 4. Dorsal view of a foot showing the typical distribution of dorsomedial and dorsolateral nerves: 1. Dorsomedial nerve of the first toe. 2. Dorsolateral nerve of the first toe. 3. Dorsomedial nerve of the second toe (yellow arrows).

A cadaveric study by Jones et al.[39] visualized an extensive arterial network forming a plexus around the first metatarsal head. This plexus, often difficult to visualize during standard surgical dissection, migrates dorsally from the FDMA and its dorsal branch and plantarly from the FPMA[14,16,39]. These arteries converge to form a plexus at the metatarsal neck, proximal to the capsular insertion (Figure 5)[14,16,30,31,38-40].

Iatrogenic vascular damage to the metatarsal head, including injury to the intramedullary and metaphyseal blood supply, can occur during surgical procedures, potentially due to excessive penetration of the Shannon burr during osteotomy[16,39,40].

The sesamoid complex

The hallux sesamoid complex, located plantar to the first MTPJ, plays a critical biomechanical role, transmitting up to 50% of body weight during normal activities and exceeding 300% during push-off[41]. The greater tibial sesamoid resides on the medial head of the FHB, while the lesser fibular sesamoid is located on the lateral head[41,42]. Both sesamoids receive tendinous insertions from the adductor and abductor hallucis muscles. The medial and lateral sesamoid ligaments, originating from the respective aspects of the metatarsal head, insert onto the corresponding aspects of the tibial and fibular sesamoids, forming part of the plantar plate of the first MTPJ[43,44]. The fibular sesamoid connects to the second metatarsal neck via the deep intermetatarsal ligament[43]. A thick intersesamoid ligament unites the tibial and fibular sesamoids, constituting the central component of the plantar plate (Figure 6)[41,45]. Accurate assessment of sesamoid subluxation in HV has historically been challenging, but its recognition is crucial to guide HV treatment[16,46]. Inadequate assessment and correction of sesamoid subluxation may increase the risk of postoperative recurrence of HV[16].

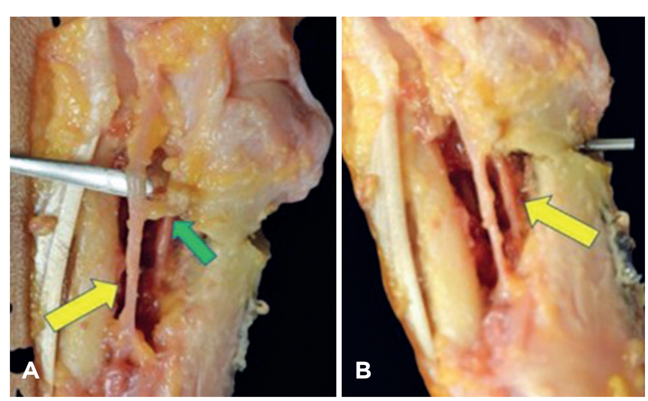

Figure 5. First metatarsal head blood supply (Macroscopically): (A) first dorsal metatarsal artery (FDMA) (yellow arrow), lateral dorsal branch of FDMA (green arrow), (B) first plantar metatarsal artery (yellow arrow).

Micro-CT assessment of the first metatarsal head vascularity

To precisely characterize the vascular architecture of the first metatarsal head, cadaveric specimens were injected with a low-viscosity radiopaque polymer and subsequently analyzed by micro-CT[14,16]. This technique provided three-dimensional visualization of the arterial network at a resolution beyond the capability of conventional imaging, mapping the intramedullary, metaphyseal, and periosteal vessels relative to the osteotomy geometry[14,16].

Micro-CT imaging confirmed that the FDMA, its lateral dorsal branch, and the FPMA form an interconnecting plexus at the metatarsal neck that migrates dorsally from above and plantarly from below, converging proximal to the capsular insertion. This plexus provides the primary intramedullary blood supply to the metatarsal head via nutrient channels that penetrate the cortex in the dorsolateral and plantar-lateral quadrants (Figure 7)[14,16].

Third- and fourth-generation MIS techniques: Anatomical considerations

Third-generation: MICA and PeICO techniques

The MICA technique, as described by Vernois and Redfern[9,10], employs a distal extra-articular Chevron-shaped osteotomy using a 20 × 2-mm Shannon burr introduced through a medial stab incision at the metatarsal neck. The osteotomy is oriented with the apex medially, creating a dorsal arm directed superiorly and a plantar arm directed inferiorly, both converging to exit the lateral cortex.

Carvalho et al.[14,16], in a cadaveric and micro-CT study of the MICA technique, provided detailed anatomical mapping of the vascular structures at risk during the Chevron-type osteotomy. From an anatomical standpoint, this study demonstrates that the dorsal arm of the osteotomy passes in close proximity to the FDMA and its lateral dorsal branch, which course dorsolaterally through the first web space and converge at

Figure 6. First metatarsal head distal aspect: (A and B) the sesamoid complex.
Source: Carvalho (2025)[16]

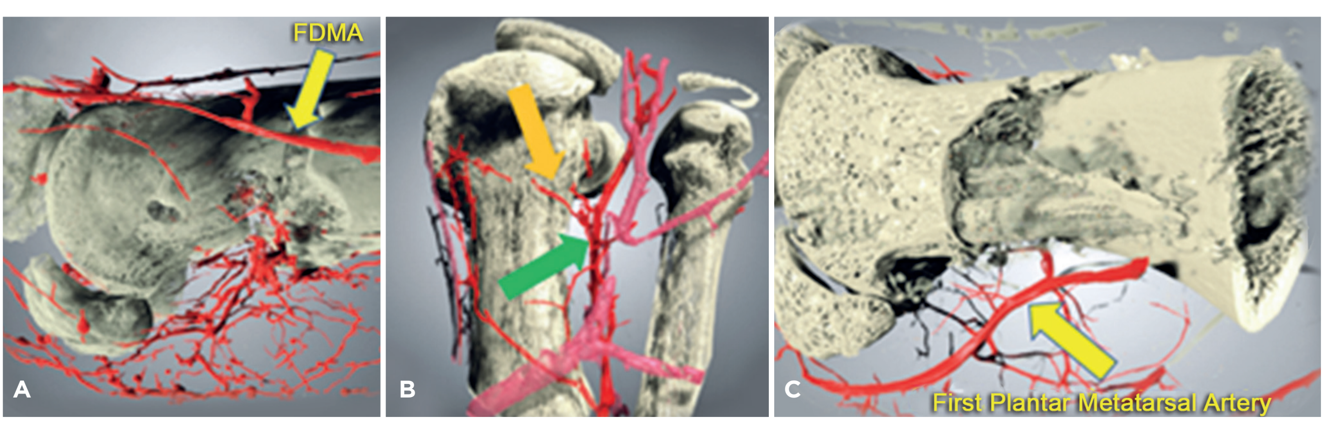

Figure 7. First metatarsal head blood supply (Micro-CT images): Lateral view (A) first dorsal metatarsal artery (FDMA) (yellow arrow), (B) antero-posterior view: Lateral dorsal branch of FDMA (orange arrow) and FDMA (green arrow), (C) oblique view: First plantar metatarsal artery (yellow arrow).
Source: Carvalho (2025)[16]

a bifurcation located a median of 25.6 mm proximal to the most distal point of the first metatarsal head. The plantar arm, in turn, runs trajectorially adjacent to the FPMA and the lateral head of the FHB, with the FPMA trifurcating into its sesamoid and metatarsal head branches at a median distance of 23.9 mm from the same distal reference point. The final phase of both arms – the moment the Shannon burr exits the lateral cortex – represents the point of maximum vascular risk, since any further advancement beyond this threshold engages the soft tissue envelope directly; micro-CT analysis established this safe penetration margin at 3.9 mm dorsolaterally (protecting the FDMA) and 4.0 mm plantar-laterally (protecting the FPMA), beyond which the arterial plexus becomes vulnerable to iatrogenic injury (Figure 8).

Del Vecchio et al.[11], in a cadaveric study on the PeICO technique for HV correction, demonstrated that the primary portal (P1) lies in close anatomical proximity to critical neurovascular and tendinous structures. The mean distance between P1 and the dorsomedial digital nerve (DMDN) was only 7.3 mm (range 1.6-10.4 mm), while its distance from the lateral border of the EHL tendon averaged 17.6 mm. Notably, the osteosynthesis portal (P2), positioned approximately 15 mm proximal and 3 mm dorsal to P1, exhibited the narrowest safety margin of the entire procedure with respect to the DMDN, with a mean distance of only 4.1-4.2 mm – identifying this portal as the site of greatest neurological risk throughout the technique. Creation of the dorsal limb of the osteotomy, oriented perpendicular to the first metatarsal diaphysis at an angle of 10 to 20 degrees from the apex, demands heightened surgical vigilance along this same trajectory, since advancement of the burr in this region brings the instrument into direct proximity with the dorsomedial neurovascular envelope, all without direct visualization of the underlying structures (Figure 9)[11].

Fourth-generation: Transverse osteotomy with rigid fixation

Fourth-generation MIS for HV, described by Lewis et al.[12] under the acronym META, substitutes the Chevron geometry with a transverse metaphyseal cut, allowing multiplanar rotational correction. Fixation is achieved with two fully threaded screws, at least one bicortical.

The anatomical risk profile of the transverse osteotomy differs from the Chevron in that the burr traverses the full transverse diameter around the metatarsal neck in a single plane, rather than in a V-shaped trajectory[12,13,14]. This means that both the FDMA (above) and the FPMA (below) are approached simultaneously during the lateral cortex exit phase (Figure 10). The absence of a well-defined apex, in theory, reduces the directional predictability of the burr's cortical exit – particularly in hands not specifically trained in MIS technique and/or without the use of industry-specific jigs designed to guide burr orientation – potentially increasing the risk of exceeding safe soft tissue margins laterally if the technique is imprecise.

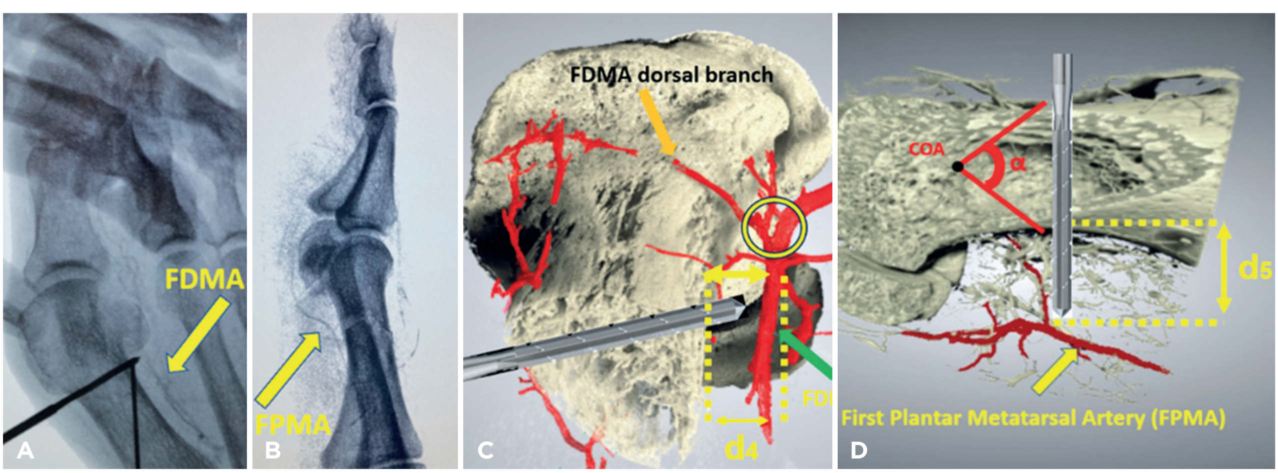

Figure 8. Vascular structures at risk during minimally invasive surgery Chevron-type osteotomy: Contrast-enhanced fluoroscopic images showing the first dorsal metatarsal artery (FDMA) (yellow arrow) (A) and first plantar metatarsal artery (FPMA) (yellow arrow) (B), and their relationship to Shannon Burr. Safe distance to advance with the Shannon Burr from the first metatarsal cortex (C) without injuring the FDMA (green arrow) (d4), and (D) to avoid injury to the FPMA (yellow arrow) (d5). (C) Distance, d4: distance between the lateral cortex exit point of the minimally invasive surgery Chevron-type osteotomy on the first metatarsal and the FDMA (dorsal plane); FDMA dorsal branch (orange arrow). (D) Distances, d5: distance between the lateral cortex exit point of the minimally invasive surgery Chevron-type osteotomy on the first metatarsal and the FPMA (plantar plane). COA: Chevron osteotomy apex (black circle); Alpha angle (α): Angle between the dorsal and the plantar arms of the minimally invasive surgery Chevron-type osteotomy.
Source: Carvalho (2025)[16]

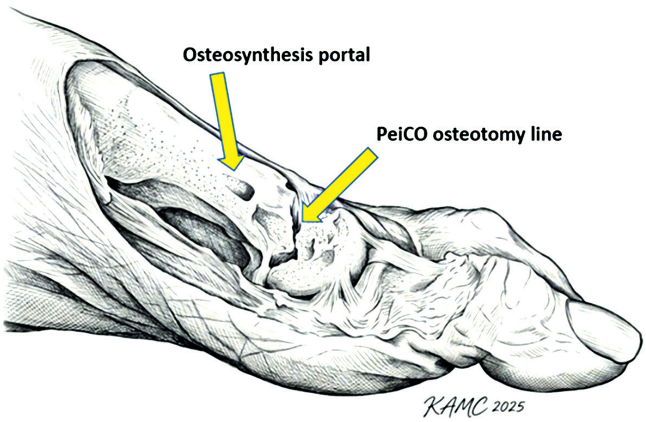

Figure 9. Schematic drawing depicting the percutaneous, intra-articular chevron osteotomy (PeICO) technique, demonstrating the chevron osteotomy line at the head of the first metatarsal and the corresponding osteosynthesis portal (yellow arrows), used for insertion of the fixation material.

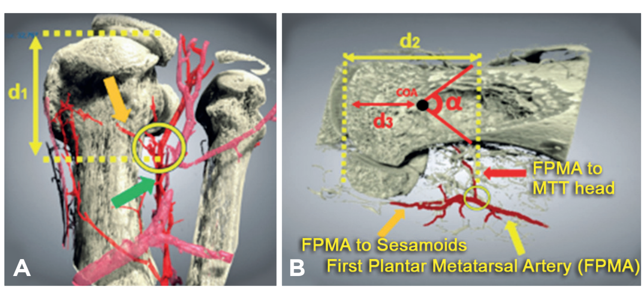

Figure 10. Safe position for performing minimally invasive surgery Chevron-type osteotomy (Micro-CT images). (A) Anteroposterior view: Anatomical reference landmarks, namely the bifurcation (inside of the yellow circle), between the first plantar metatarsal artery (FDMA) (green arrow) and the Lateral Dorsal Branch of the FDMA (orange arrow), along with the most distal portion of the first metatarsal head. (B) Lateral view: Anatomical reference landmarks, namely the trifurcation (inside of the yellow circle), between the FPMA (yellow arrow) and its branches to sesamoids (orange arrow) and the first metatarsal head (red arrow). (B) COA: Chevron osteotomy apex (black circle); Alpha angle (α): Angle between the dorsal and the plantar arms of the minimally invasive surgery Chevron-type osteotomy. (A) Distance, d1: between the most distal point of the first metatarsal head and the bifurcation of the FDMA and its lateral dorsal branch. (B) Distances, d2: between the most distal point of the first metatarsal head and the trifurcation between the FPMA and its branches to the sesamoids and the first metatarsal head; and d3: between the metatarsal neck's flare and the most distal point of the first metatarsal head.

Source: Carvalho (2025)[16]

Biomechanical studies have shown no significant difference in ultimate load or stiffness between third- and fourth-generation MIS constructs, and comparative radiographic outcome studies have found no significant difference in angular correction[48]. The choice between geometries should therefore be guided principally by surgeon familiarity and comfort, rather than perceived biomechanical superiority[12,13,48-50].

Quantitative safe zones for MIS third- and fourth-generation osteotomy

The determination of safe operating distances – measured by defined fluoroscopic landmarks – is the primary practical contribution of the cadaveric and micro-CT studies reviewed here[14,16]. These distances were established from a population of 20 cadaveric specimens with HV, all undergoing standardized MIS Chevron-type osteotomy with a 20 × 2-mm Shannon burr.

Safe distances from the distal metatarsal head

Two key safe distances were defined, both measured from the most distal point of the first metatarsal head articular surface on lateral fluoroscopic imaging (Figure 10)[14,16]:

- **Dorsal arm:** a median safe distance of 25.6 mm. The dorsal arm of the osteotomy – where the Shannon burr exits the dorsolateral cortex – should be completed at or proximal to this distance from the metatarsal head tip, since osteotomies extending distal to this threshold approach the FDMA and its dorsal branch, increasing the risk of vascular injury.
- **Plantar arm:** a median safe distance of 23.9 mm. The plantar arm should likewise terminate at or proximally to this point relative to the metatarsal head, as extension beyond this threshold places the FPMA at increasing risk of injury.

These distances imply that the plantar landmark sits slightly more distal than the dorsal landmark, reflecting the differing courses of the FPMA and FDMA relative to the metatarsal neck. In a Chevron-type configuration, because the osteotomy is angulated (alpha angle ≈124 degrees)[9,10,14], the dorsal and plantar limbs are geometrically distinct cuts, each requiring independent verification against its respective vascular landmark.

Safe lateral excursion of the Shannon burr

A complementary set of safety margins governs the lateral advancement of the Shannon burr beyond the lateral cortex exit point, reflecting the soft tissue clearance available between the cortical surface and the FDMA (dorsally) and FPMA (plantarly) (Figure 8C and D):

- **Dorsolateral excursion**: maximum 3.9 mm beyond the lateral cortex exit point. Beyond this distance, the FDMA and/or its dorsal branch are at risk of direct laceration.

- **Plantar-lateral excursion:** maximum 4.0 mm beyond the lateral cortex exit point. Beyond this limit, the FPMA and the lateral aspect of the FHB are at imminent risk.

Adherence to these excursion limits is particularly relevant given that the surgeon assesses burr position through a two-dimensional fluoroscopic projection; the dorsolateral and plantar-lateral soft tissue dimensions are not directly visualized intraoperatively, making pre-operative knowledge of these safe zones essential rather than supplementary[14,16].

Extrapolating the safe-zone concept to the fourth-generation transverse osteotomy (META)

The safe distances described above were derived specifically from a chevron-type (angulated, V-shaped) osteotomy, in which the dorsal and plantar limbs diverge from a proximal apex and therefore exit the cortex at two distinct sagittal levels.

The META technique, by contrast, uses a single-plane transverse (non-angulated) osteotomy at the metatarsal neck, with only a minor 10-degree proximal-to-distal tilt introduced to compensate for burr-associated shortening[12]. Because the cut is performed in one plane rather than as two diverging limbs, the dorsal and plantar cortical exit points of a transverse osteotomy lie essentially at the same distance from the metatarsal head – unlike the chevron, where the geometry of the two arms separates the dorsal and plantar exit levels.

This distinction has a direct anatomical implication. If a transverse osteotomy is performed at approximately 26 mm from the most distal point of the first metatarsal head articular surface, it would simultaneously satisfy – within a single cut – both vascular safety thresholds identified by Carvalho et al.[14]: it lies at or proximal to the 23.9-mm plantar limit (protecting the FPMA) and closely approximates the 25.6-mm dorsal limit (protecting the FDMA and its dorsal branch). In effect, the transverse geometry of META removes the need to reconcile two separate arm-specific distances, since one plane can be positioned to respect both vascular landmarks concurrently (Figure 11).

We propose that this represents a logical anatomical extrapolation of the safe-zone concept originally described for Chevron-type (MICA) osteotomies to the fourth-generation transverse (META) technique, given that both procedures address the same extracapsular metaphyseal segment of the first metatarsal neck and rely on comparable burr dimensions (2.0-2.2 mm). However, this extrapolation has not yet been directly validated by micro-CT or perfusion studies performed on specimens using the transverse META configuration itself.

Future cadaveric micro-CT work replicating the META osteotomy – rather than the Chevron – would be valuable to confirm whether the 26-mm threshold, and the corresponding burr excursion limits (3.9 mm dorsolaterally, 4.0 mm plantar-laterally), hold true when applied to a single transverse cutting plane rather than an angulated one.

Practical landmarks and technical recommendations

The following technical recommendations are derived from the anatomical findings reviewed and are applicable to both third- and fourth-generation MIS techniques:

1. **Osteotomy apex placement.** Used for the MICA technique, the apex of the Chevron osteotomy (COA) should be positioned at the metatarsal neck flare[9,10,14], verified fluoroscopically. A too-distal apex brings both osteotomy arms closer to the arterial plexus. On lateral fluoroscopy, the COA should appear at or proximally to the mid-neck level (Figure 10B).

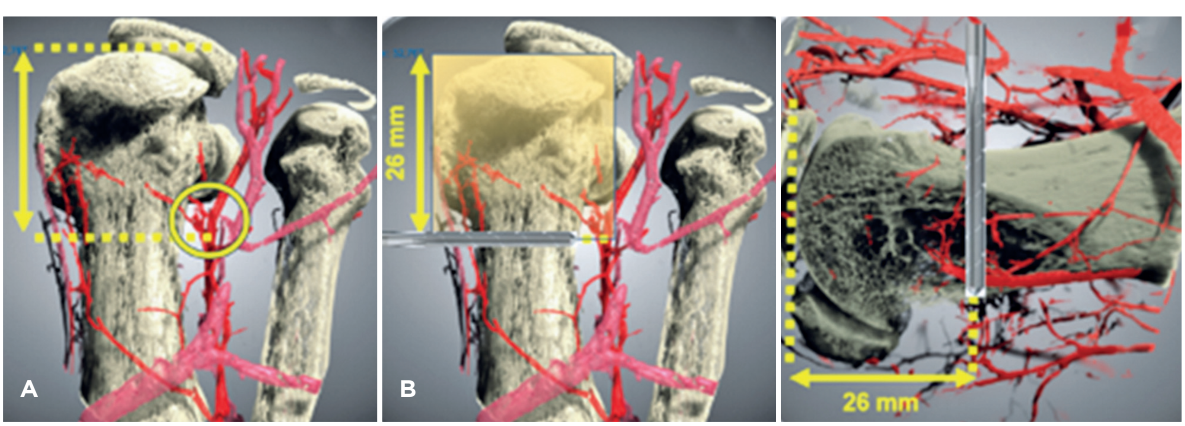

Figure 11. Theoretical safe position for performing minimally invasive surgery META osteotomy (Micro-CT images): (A) Anatomical reference landmarks, namely the bifurcation between the first plantar metatarsal artery (FDMA) and the lateral dorsal branch of the FDMA (inside the yellow circle), along with the most distal portion of the first metatarsal head. The theoretical safe position to complete the minimally invasive surgery META osteotomy is 26 mm, extending from the most distal point of the head of the first metatarsal proximally. (B) anterior view (C) lateral view.

2. **Shannon burr control.** The burr should be advanced with consistent pressure and withdrawn immediately upon tactile sensation of cortical exit. Continued advancement after cortical breakthrough directly violates the excursion safety margins. The 20 × 2-mm burr geometry provides a defined cutting width; awareness of its full width is necessary to prevent inadvertent injury at the far edge (Figure 8).
3. **Plantar arm caution.** The plantar arm carries the highest risk for FHB injury[14,16]. Maintaining a slight plantar-to-dorsal inclination during the plantar cut, rather than a purely horizontal trajectory, reduces the risk of engaging the FHB belly plantar to the osteotomy plane (Figure 8D/10B).
4. **Dorsal arm and nerve protection.** The dorsomedial nerve is most at risk when the incision portal or the burr trajectory deviates medially. The medial stab incision for the osteotomy should be placed in a strictly medial position at the metatarsal neck, avoiding any dorsalward displacement[16]. Malagelada et al.[34], in a cadaveric study, focused on increasing the safety of MIS hallux surgery, introduced the clock method and found that the dorsomedial nerve of the first toe was consistently located between 12 and 2 o'clock (0° and 60°, respectively) on the dorsomedial aspect of the hallux in right feet, and between 10 and 12 o'clock (300° and 360°, respectively) in left feet. Conversely, the dorsolateral nerve of the first toe was consistently found between 10 and 12 o'clock on the dorsolateral aspect of the hallux in the right feet and between 12 and 2 o'clock in the left foot[33,34].

First metatarsal head cartilage and tibial posterior tendon

Although not explored in the literature, two additional points of caution merit attention in this review, as they may help minimize iatrogenic injury during MIS – specifically the MICA and META techniques. In our cadaveric studies, we observed one instance of cartilage injury to the first metatarsal head resulting from excessive and inadvertent advancement of the drill, producing a 4.41 mm lesion (Figure 12A). A second point concerns the surgeon's attention to the drill's entry position: an entry angle directed too steeply from dorsal to plantar risks injury to the dorsal nerve, whereas an angle directed too steeply from plantar to dorsal risks injury to the insertion of the posterior tibial tendon (Figure 12B). Based on these observations, we recommend that both the surgical incision and the drill entry point be aligned parallel to the long axis of the first metatarsal.

Conclusion

Third- and fourth-generation MIS HV surgeries operate within an anatomical corridor containing structures invisible to the surgeon, requiring precise mastery of quantitative anatomical boundaries as the primary safeguard against iatrogenic injury. Cadaveric dissection and micro-CT vascular mapping studies establish that the Chevron osteotomy must be performed at a minimum distance of 25.6 mm (dorsal limb) and 23.9 mm (plantar limb) from the most distal point of the first metatarsal articular surface, with the excursion of the Shannon burr limited to 3.9 mm and 4.0 mm beyond the exit point on the lateral cortex. The fourth-generation META technique simultaneously addresses the FDMA and FPMA in a single transverse plane; for this technique, a unified safety distance of approximately 26 mm is proposed, although this measurement still awaits specific validation through anatomical and micro-CT studies. Neurological risk for both osteotomy generations centers on the dorsomedial nerve of the first toe. Biomechanical and radiographic equivalence between third- and fourth-generation constructs confirms that the choice of technique should be based on surgical training rather than alleged mechanical superiority, and that safe execution – regardless of geometry – depends on mastering the anatomical risk zones described in this review.

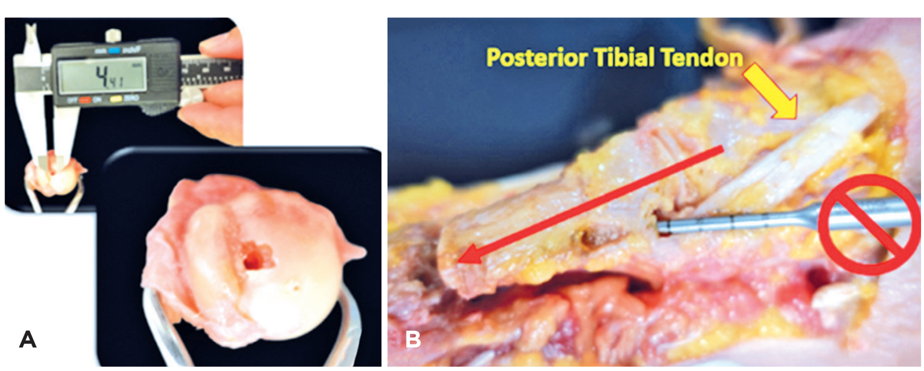

Figure 12. (A) Cartilage injury on the head of the first metatarsal resulting from excessive and inadvertent advancement of drills, measuring 4.41 mm on a digital caliper. (B) Dissection demonstrating the ideal drill entry trajectory, following the long axis of the first metatarsal (long red arrow). An entry angle that is excessively steep in the plantar-to-dorsal direction (prohibition symbol) carries a risk of injury to the posterior tibial tendon (yellow arrow).

Authors' contributions: Each author contributed individually and significantly to the development of this article: KAMC *(https://orcid.org/0000-0003-1082-6490) Wrote the article, participated in the review process; SF *(https://orcid.org/0009-0008-9631-8481), AF *(https://orcid.org/0000-0002-3905-9662), and MDP *(https://orcid.org/0000-0001-6043-698X) Participated in the review process. All authors read and approved the final manuscript. *ORCID (Open Researcher and Contributor ID).

References

1. Cai Y, Song Y, He M, He W, Zhong X, Wen H, Wei Q. Global prevalence and incidence of hallux valgus: a systematic review and meta-analysis. J Foot Ankle Res. 2023;16(1):63.
2. Nix S, Smith M, Vicenzino B. Prevalence of hallux valgus in the general population: a systematic review and meta-analysis. J Foot Ankle Res. 2010;3:21.
3. Carvalho KAM, Behrens A, Mallavarapu V, Jasper R, Mansur NSB, Lalevee M, et al. Automated three-dimensional distance and coverage mapping of hallux valgus: a case-control study. J Foot Ankle. 2022;16(1):41-5.
4. Lalevée M, Barbachan Mansur NS, Lee HY, Maly CJ, Iehl CJ, Nery C, et al. Distal Metatarsal Articular Angle in Hallux Valgus Deformity. Fact or Fiction? A 3-Dimensional Weightbearing CT Assessment. Foot Ankle Int. 2022;43(4):495-503.
5. Smyth NA, Aiyer AA. Introduction: why are there so many different surgeries for hallux valgus? Foot Ankle Clin. 2018;23:171-82.
6. Alimy AR, Polzer H, Ocokoljic A, Ray R, Lewis TL, Rolvien T, et al. Does Minimally Invasive Surgery Provide Better Clinical or Radiographic Outcomes Than Open Surgery in the Treatment of Hallux Valgus Deformity? A Systematic Review and Meta-analysis. Clin Orthop Relat Res. 2023;481(6):1143-55.
7. Gonzalez T, Encinas R, Johns W, Benjamin Jackson J 3rd. Minimally Invasive Surgery Using a Shannon Burr for the Treatment of Hallux Valgus Deformity: A Systematic Review. Foot Ankle Orthop. 2023;8(1):24730114221151069.
8. Del Vecchio JJ, Ghioldi ME. Evolution of Minimally Invasive Surgery in Hallux Valgus. Foot Ankle Clin. 2020;25(1):79-95.
9. Vernois J, Redfern D. Percutaneous chevron the union of classic stable fixed approach and percutaneous technique. Fuss Sprunggelenk. 2013;11(2):70-5.
10. Redfern D, Vernois J. Minimally invasive chevron Akin (MICA) for correction of hallux valgus. Tech Foot Ankle Surg. 2016;15:3-11.
11. Del Vecchio JJ, Ghioldi ME, Uzair AE, Chemes LN, Manzanares-Céspedes MC, Dealbera ED, et al. Percutaneous, Intra-articular, Chevron Osteotomy (PeICO) for the Treatment of Hallux Valgus: A Cadaveric Study. Foot Ankle Int. 2019;40(5):586-95.
12. Lewis TL, Lau B, Alkhalfan Y, Trowbridge S, Gordon D, Vernois J, et al. Fourth-Generation Minimally Invasive Hallux Valgus Surgery With Metaphyseal Extra-Articular Transverse and Akin Osteotomy (META): 12 Month Clinical and Radiologic Results. Foot Ankle Int. 2023;44(3):178-91.
13. Carvalho KAM, Baptista AD, de Cesar Netto C, Johnson AH, Dalmau-Pastor M. Minimally invasive chevron-Akin for correction of moderate and severe hallux valgus deformities: clinical and radiologic outcomes with a minimum 2-year follow-up. Foot Ankle Int. 2022;43(10):1317-30.
14. Carvalho KAM, Fayed A, Barbachan Mansur NS, Godoy-Santos AL, Talusan P, Chrea B, et al. Anatomical and Micro-CT Assessment of the First Metatarsal Head Vascularization and Soft Tissue Envelope Following Minimally Invasive Chevron Osteotomy for Hallux Valgus Deformity. Foot Ankle Int. 2025;46(1):102-14.
15. Nunes GA, de Carvalho KAM, Ferreira GF, Filho MVP, Baptista AD, Zambelli R, et al. Minimally invasive Chevron Akin (MICA) osteotomy for severe hallux valgus. Arch Orthop Trauma Surg. 2023;143(9):5507-14.
16. Carvalho KAM. Minimally Invasive Chevron-Akin osteotomy for Correction of Moderate and Severe Hallux Valgus Deformities: An Anatomical, Clinical and Radiological Study [thesis]. Barcelona: Universitat de Barcelona; 2025.
17. Dalmau-Pastor M, Yasui Y, Calder JD, Karlsson J, Kerkhoffs GM, Kennedy JG. Anatomy of the inferior extensor retinaculum and its role in lateral ankle ligament reconstruction: a pictorial essay. Knee Surg Sports Traumatol Arthrosc. 2016;24(4):957-62.
18. Ho B, Khan Z, Switaj PJ, Ochenjele G, Fuchs D, Dahl W, et al. Treatment of peroneal nerve injuries with simultaneous tendon transfer and nerve exploration. J Orthop Surg Res. 2014;9:67.
19. Zielinska N, Tubbs RS, Ruzik K, Olewnik Ł. Classifications of the extensor hallucis longus tendon variations: Updated and comprehensive narrative review. Ann Anat. 2021;238:151762.
20. Standring S, Tubbs RS. Gray's Anatomy: The Anatomical Basis of Clinical Practice. Int Ed. Elsevier; 2016.
21. Maddox MB, Mashaw SA, MacDonald EM, Mira AJ, Parker WJ, Fakoya AO. Four Tendinous Slips of Flexor Hallucis Longus Tendon: A Case Report. Cureus. 2024;16(5):e59601.
22. Feng SM, Sun QQ, Wang AG, Fan JQ. Flexor Hallucis Longus Tendon Impingement Syndrome: All-inside Arthroscopic Treatment and Long-term Follow-up. J Foot Ankle Surg. 2020;59(6):1197-200.
23. Hamel AJ, Donahue SW, Sharkey NA. Contributions of active and passive toe flexion to forefoot loading. Clin Orthop Relat Res. 2001(393):326-34.
24. Bartosiak K, McCormick JJ. Avascular Necrosis of the Sesamoids. Foot Ankle Clin. 2019;24(1):57-67.
25. Hakim-Zargar M, Aronow MS, Gibson L, Obopilwe E. Implications for the anatomy of the flexor hallucis brevis insertion. Foot Ankle Int. 2010;31(1):65-8.
26. Barták V, Hromádka R, Fulín P, Jahoda D, Sosna A, Popelka S. Anatomical study of flexor hallucis brevis insertion: Implications for clinical practice. Acta Chir Orthop Traumatol Cech. 2011;78(2):145-8. Czech
27. Chittoria RK, Pratap H, Yekappa SH. Abductor Hallucis: Anatomical Variation and Its Clinical Implications in the Reconstruction of Chronic Nonhealing Ulcers and Defects of Foot. Adv Wound Care. 2015;4(12):719-23.
28. Agawany AE, Meguid EA. Mode of insertion of the abductor hallucis muscle in human feet and its arterial supply. Folia Morphol (Warsz). 2010;69(1):54-61.
29. Owens S, Thordarson DB. The adductor hallucis revisited. Foot Ankle Int. 2001;22(3):186-91.

30. Sarrafian SK KA. Sarrafian's anatomy of the foot and ankle: descriptive, topographic, functional. Philadelphia: Lippincott; 1993.
31. Kelikian AS, Sarrafian SK. Sarrafian's anatomy of the foot and ankle: descriptive, topographic, functional. Fourth edition. ed. Philadelphia: Wolters Kluwer; 2024.
32. Hacking C KO. Adductor hallucis muscle. Radiopaedia [Internet]. 2016. Available from: https://doi.org/10.53347/rID-44461.
33. Dalmau-Pastor M, Vega J, Malagelada F, Peña F, Manzanares-Céspedes MC. An Anatomical Study of Nerves at Risk During Minimally Invasive Hallux Valgus Surgery. J Vis Exp. 2018(132):56232.
34. Malagelada F, Dalmau-Pastor M, Fargues B, Manzanares-Céspedes MC, Peña F, Vega J. Increasing the safety of minimally invasive hallux surgery – An anatomical study introducing the clock method. Foot Ankle Surg. 2018;24(1):40-4.
35. Inchai C, Vaseenon T, Tanaka Y, Mahakkanukrauh P. The distribution pattern of the dorsal cutaneous nerves of the foot and its clinical implications. Anat Cell Biol. 2020;53(2):137-42.
36. Dalmau-Pastor M, Malagelada F, Cordier G, Del Vecchio JJ, Ghioldi ME, Vega J. Anatomical Study of Minimally Invasive Lateral Release Techniques for Hallux Valgus Treatment. Foot Ankle Int. 2020;41(8):984-92.
37. Solan MC, Lemon M, Bendall SP. The surgical anatomy of the dorsomedial cutaneous nerve of the hallux. J Bone Joint Surg Br. 2001;83(2):250-2.
38. Shereff MJ, Yang QM, Kummer FJ. Extraosseous and intraosseous arterial supply to the first metatarsal and metatarsophalangeal joint. Foot Ankle. 1987;8(2):81-93.
39. Jones KJ, Feiwell LA, Freedman EL, Cracchiolo A 3rd. The effect of chevron osteotomy with lateral capsular release on the blood supply to the first metatarsal head. J Bone Joint Surg Am. 1995;77(2):197-204.
40. Malal JJ, Shaw-Dunn J, Kumar CS. Blood supply to the first metatarsal head and vessels at risk with a chevron osteotomy. J Bone Joint Surg Am. 2007;89(9):2018-22.
41. Dedmond BT, Cory JW, McBryde A, Jr. The hallucal sesamoid complex. J Am Acad Orthop Surg. 2006;14(13):745-53.
42. McBryde AM, Jr., Anderson RB. Sesamoid foot problems in the athlete. Clin Sports Med. 1988;7(1):51-60.
43. Jahss MH. The sesamoids of the hallux. Clin Orthop Relat Res. 1981(157):88-97.
44. Frankel JP, Harrington J. Symptomatic bipartite sesamoids. J Foot Surg. 1990;29(4):318-23.
45. Richardson EG. Injuries to the hallucal sesamoids in the athlete. Foot Ankle. 1987;7(4):229-44.
46. Katsui R, Samoto N, Taniguchi A, Akahane M, Isomoto S, Sugimoto K, et al. Relationship Between Displacement and Degenerative Changes of the Sesamoids in Hallux Valgus. Foot Ankle Int. 2016;37(12):1303-9.
47. Lewis TL, Barakat A, Mangwani J, Ramasamy A, Ray R. Current concepts of fourth-generation minimally invasive and open hallux valgus surgery. The Bone & Joint Journal. 2025;107-B(1):10-8.
48. Aiyer A, Massel DH, Siddiqui N, Acevedo JI. Biomechanical Comparison of 2 Common Techniques of Minimally Invasive Hallux Valgus Correction. Foot Ankle Int. 2021;42(3):373-80.
49. Acevedo JI, Garcia AR, Queen JD, McWilliam JR. Fourth generation hallux valgus correction. Tech Foot Ankle Surg. 2024;23(2):68-77.
50. Loder BG, Lucas J, Bergeron M. Third generation versus fourth generation percutaneous hallux valgus correction: A radiographic analysis of outcomes. J Foot Ankle Surg. 2025;64(1):42-4.